Magnetohydrodynamic Flow Past a Thin Airfoil

E. CUMBERBATCH,* L. SARASON,† AND H. WEITZNER‡
Courant Institute of Mathematical Sciences, New York University, New York, N. Y.

The steady flow of a perfectly conducting magnetohydrodynamic fluid past a thin nonconducting airfoil is studied with the usual model in which the fluid variables obey the Lundquist equations linearized about a constant unperturbed flow. "Hyperliptic" flows, in which hyperbolic and elliptic fields are superimposed, are considered. Results of Grad, McCune and Resler, and Sears and Resler are extended and considered in detail for the case of an arbitrarily inclined unperturbed field. The general solution contains four line singularities along the characteristics through the ends of the body and has two arbitrary constants. By a "generalized Kutta-Joukowski condition," these constants are fixed so that two of the line singularities disappear. Specifically, it is required that the solution be locally square integrable. Behavior of the exponents of the singularities is investigated by numerical computation and, in limiting cases, analytically. The singular parts of some flows are investigated numerically.

I. Introduction

THE standard mathematical model for the study of the steady flow of a perfectly conducting magnetohydrodynamic fluid past a nonconducting airfoil consists of the Lundquist equations linearized about constant unperturbed fluid velocity, density, and magnetic field together with the appropriate boundary conditions.[1, 2] Essentially two distinct types of flows appear, loosely corresponding to "subsonic" and "supersonic" flows of fluid dynamics. Since the regime similar to subsonic flow possesses properties common to both subsonic and supersonic flows, the situation is more complex than either of the two fluid dynamic cases. With the methods outlined by Grad,[2] this paper examines the "hyperliptic" flows[1] in some detail and extends the results to cases not considered previously. In much of the work presented, all vectors are considered to have three components, although they are functions of two space variables only. Some sections are restricted to the cases where vectors are two-dimensional and where the unperturbed flow and magnetic field have a special orientation.

In the next section the problem is formulated, Grad's results[2] are given, and the hyperliptic regime is described. In Sec. 3 the problem is reduced to the solution of a singular integral equation with nonunique solutions.

Similar to subsonic fluid dynamics, functions that are singular at the ends of the body, may be added to any solution, by which means the singularities in the solution at either end of the body may be suppressed. The dual nature of the hyperliptic regime is evident in the fact that the singularities on the body also are propagated into the fluid along the real characteristics. This feature is used in Sec. 4 to obtain a physically acceptable uniqueness condition analogous to the Kutta-Joukowsky condition of fluid dynamics.[3] The condition proposed insures the square integrability of the flow variables over any region of the fluid. The line singularities remaining in the solution imply a breakdown of the linear analysis used, and the solutions in the neighborhood of these singularities may not provide good pointwise approximations to the correct solution. On the other hand, they may give an indication of the formation of shocks.

Since the exponents of the singularities are complicated functions of the flow parameters, numerical values were obtained. As described in Sec. 5, the exponents were found over the whole hyperliptic regime for a set of flow parameters, and the regimes in which the trailing and leading edge singularities are to be removed could be separated. In the strictly two-dimensional problem, a singularity is left at either the leading edge or the trailing edge. In the limit of vanishing magnetic field, this singularity is at the leading edge, and hence the ordinary Kutta-Joukowsky condition is obtained. In the general problem, a singularity is left at each other edge. The exponent of the singularity in the solution of the restricted problem is not obtained as a uniform limit of the corresponding exponents in the solution of the general problem, for it may be a limit of either of the exponents in the general problem. The singular flow near the edges of the body was computed for several cases of the restricted problem, and the results are given in Sec. 6.

II. Formulation of the Problem

The steady-state equations for a perfectly conducting plasma, when linearized about a constant flow $\bar{U}_0$, magnetic field $\bar{B}_0$, density ρ_0, sound speed a_0, and magnetic permeability μ, are

$$(\bar{U}_0\cdot\bar{\nabla})\rho + \rho_0\bar{\nabla}\cdot\bar{u} = 0 \tag{1a}$$

$$\rho_0(\bar{U}_0\cdot\bar{\nabla})u + a_0^2\bar{\nabla}\rho - (1/\mu)(\bar{\nabla}\times\bar{B})\times\bar{B}_0 = 0 \tag{1b}$$

$$(\bar{U}_0\cdot\bar{\nabla})\bar{B} - \bar{\nabla}\times(\bar{u}\times\bar{B}_0) = 0 \tag{1c}$$

$$\bar{\nabla}\cdot\bar{B} = 0 \tag{1d}$$

Since only flows depending on two space variables are considered, the gradient operator may be chosen as $(\partial/\partial x, \partial/\partial y, 0)$. Furthermore, the vectors $\bar{U}_0$ and $\bar{B}_0$ are chosen as

$$\bar{U}_0 = U_0(1, 0, 0) \tag{2a}$$

$$\bar{B}_0 = B_0(\cos\theta, \sin\theta, b) \tag{2b}$$

where U_0 and B_0 are the magnitude projections of $\bar{U}_0$ and $\bar{B}_0$ into the xy plane, and it is assumed that $0 < \theta < \pi$. (The case $\sin\theta = 0$ is degenerate and is not considered here.) As written, the system (1) has eight equations but only seven unknowns. The system of equations actually used consists of (1) with the x component of (1c) replaced by the condition that the perturbed flow variables vanish as $x \to \pm\infty$ for y fixed. Under this condition, the omitted equation may be derived easily from the remaining equations.

The y component of (1c) may be integrated immediately, and with the same assumption on behavior at infinity, it follows that

$$B_0\cos\theta u_y - U_0B_y - B_0\sin\theta u_x = 0 \tag{3}$$

Received by IAS August 27, 1962; revision received November 13, 1962. The work presented in this paper was supported by the Air Force Office of Scientific Research under Contract AF-49(638)-1006.

* Now at the Department of Mathematics, University of Leeds, England.
† Assistant Research Scientist.
‡ Assistant Professor of Mathematics.

Thus u_x may be eliminated in terms of u_y and B_y. With the introduction of nondimensional variables defined by

$$\bar{u} = U_0(u, v, w) \tag{4a}$$

$$\bar{B} = B_0(\xi, \eta, \zeta) \tag{4b}$$

$$\rho = \rho_0\sigma \tag{4c}$$

and on the definition of the Alfven speed, $A_0^2 = B_0^2/\mu\rho_0$, the basic equations become

$$\sin\theta \frac{\partial\sigma}{\partial x} + \cos\theta \frac{\partial v}{\partial x} + \sin\theta \frac{\partial v}{\partial y} - \frac{\partial\eta}{\partial x} = 0 \tag{5a}$$

$$a_0^2 \sin\theta \frac{\partial\sigma}{\partial x} + U_0^2 \cos\theta \frac{\partial v}{\partial x} + (A_0^2 \sin^2\theta - U_0^2) \frac{\partial\eta}{\partial x} - A_0^2 \sin^2\theta \frac{\partial\xi}{\partial y} = -bA_0^2 \sin\theta \frac{\partial\zeta}{\partial x} \tag{5b}$$

$$a_0^2 \sin\theta \left(\cos\theta \frac{\partial\sigma}{\partial x} + \sin\theta \frac{\partial\sigma}{\partial y}\right) + U_0^2 \frac{\partial v}{\partial x} - U_0^2 \cos\theta \times \frac{\partial\eta}{\partial x} = -bA_0^2 \sin\theta \left(\cos\theta \frac{\partial\zeta}{\partial x} + \sin\theta \frac{\partial\zeta}{\partial y}\right) \tag{5c}$$

$$\frac{\partial\xi}{\partial x} + \frac{\partial\eta}{\partial y} = 0 \tag{5d}$$

and

$$U_0^2 \frac{\partial w}{\partial x} - A_0^2 \left(\cos\theta \frac{\partial\zeta}{\partial x} + \sin\theta \frac{\partial\zeta}{\partial y}\right) = 0 \tag{6a}$$

$$\sin\theta \left(\cos\theta \frac{\partial w}{\partial x} + \sin\theta \frac{\partial w}{\partial y}\right) - \sin\theta \frac{\partial\zeta}{\partial x} - b\left(\cos\theta \frac{\partial v}{\partial x} + \sin\theta \frac{\partial v}{\partial y} - \frac{\partial\eta}{\partial x}\right) = 0 \tag{6b}$$

(and $u \sin\theta = v \cos\theta - \eta$). If $b = 0$, the variables w and ζ disappear from (5), and the system decouples into two independent sets, (5) and (6). In the strictly two-dimensional problem, the variables w and ζ are ignored, for (6) with appropriate boundary conditions is solved easily.

The general method of solving the full equations is to express all the variables in terms of their values on the boundary of the body and then to use the relations among the variables to obtain equations for the boundary values. In the hyperbolic regime algebraic relations result, whereas in the hyperliptic regime integral equations appear. In order to formulate the boundary conditions, an essential part of the statement of the problem, it is necessary to study the solutions of the system (5) and (6). This discussion also will include the first step in the reduction of the problem to relations among the boundary values.

As described by Grad, the system (5) and (6) may readily be reduced to characteristic form. One attempts to determine a constant λ and a linear combination of the variables $Z(x, y)$, $Z = c_1\sigma + c_2v + c_3w + c_4\xi + c_5\eta + c_6\zeta$, such that Z satisfies the equation

$$[(\partial/\partial x) - (1/\lambda)(\partial/\partial y)]Z = 0 \tag{7}$$

Such a linear combination (called a Riemann invariant) exists if and only if λ satisfies the algebraic equation

$$0 = \{(1 + \lambda^2)(\cos\theta + \lambda \sin\theta)^2 - (1 + \lambda^2)[M_0^2 + m_0^2(1 + b^2)] + m_0^2M_0^2\}[(\lambda \sin\theta + \cos\theta)^2 - M_0^2] \tag{8}$$

where the constants m_0 and M_0 are defined by $m_0 = U_0/a_0$, $M_0 = U_0/A_0$. For the real values of λ satisfying (8), there are real linear combinations Z satisfying (7). For such real λ, (7) states that Z is constant on the characteristic lines $x + \lambda y = C$. Thus, $Z(x,y)$ is given throughout the fluid in terms of its values on the airfoil (or at infinity). The complex roots of (8) generate complex linear combinations. In the latter case, (7) is essentially equivalent to the Cauchy-Riemann equations and states that Z is an analytic function of the complex variable $(x + \lambda y)$. When all the roots of (8) are real, the flow is hyperbolic; when some of the roots are real and some are complex, the flow is called hyperliptic. There are no other possibilities.

The second factor of (8) always has two real roots, and the nature of the roots of the first factor may be obtained by the simple graphical construction described by Grad (see Fig. 1). Each real tangent from the point $-\bar{U}_0$ to the characteristic cone of the time-dependent system of differential equations generates the direction of the characteristic lines, along which some Z is constant, and a positive direction along such lines. This direction is from $-\bar{U}_0$ to the curve. For a given characteristic, the positive direction is called "downstream," because it is the direction of the propagation values of Z for the time-dependent problem. Correspondingly, the negative direction is called "upstream." The terms "upstream" and "downstream," as defined here, need not agree with the usual definition in terms of direction of mass flow. However, the terms are relevant in that it is at the upstream ends of characteristics at which boundary conditions should be applied. It easily is seen from Fig. 1 that there is always at least one real tangent to each of the two inner wave-fronts. When $-\bar{U}_0$ is between the inner and outer wave-fronts, there are only these two real tangents. Hence the first factor of (8) must have two complex conjugate roots, and the flow is hyperliptic. Elsewhere there are four real tangents, and the flow is hyperbolic. For the rest of this paper, only hyperliptic flows are considered.

The explicit forms for the various Riemann invariants are given by Grad and are exhibited below. It is convenient to consider a vector with six components:

$$\mathbf{P} = (\sigma/m_0^2, v, \xi, \eta, \zeta, w) \tag{9}$$

and represent the invariants as

$$Z_i = \mathbf{r}_i \cdot \mathbf{P} \qquad i = 1, 2, 3, 4, 5, 6 \tag{10}$$

The two invariants associated with the quadratic factor of (8) are given by ($\mathbf{r}_5 = \mathbf{r}_+$, $r_6 = \mathbf{r}_-$)

$$\mathbf{r}_\pm = \left(1, 0, \pm\frac{1}{M_0^2}, \mp\frac{\lambda_\pm}{M_0^2}, \frac{b}{M_0^2}, 0\right) + \left[\cos\theta \pm M_0\left(\frac{\tan^2\theta(1 + \lambda_\pm^2)}{(1 + \lambda_\pm^2 \tan\theta)^2} - 1\right)\right] \times \left(0, -\csc\theta, 0, 0, \pm\frac{1}{bM_0}, \frac{1}{b}\right) \tag{11}$$

where

$$\lambda_\pm = (\pm M_0 - \cos\theta) \csc\theta \tag{12}$$

The four other invariants may be expressed conveniently in terms of the parameters defined by

$$\tan\phi = \lambda \tag{13}$$

$$\delta = \theta - \phi \tag{14}$$

so that

$$\cos^2\delta_i - \cos^2\phi_i[M_0^2 + (1 + b^2)m_0^2] + m_0^2M_0^2 \cos^4\phi_i = 0 \qquad i = 1, 2, 3, 4 \tag{15}$$

and

$$\mathbf{r}_i = [M_0^2 \sin\phi_i \cos^2\phi_i - \sin\theta \cos\delta_i,\ \cos\phi_i(1 - M_0^2 \cos^2\phi_i),$$
$$- \cos^2\phi_i \sin\delta_i,\quad \sin\phi_i \cos\phi_i \sin\delta_i,$$
$$b \cos^2\phi_i \sin\phi_i,\quad b \cos\phi_i \sin\theta] \quad (16)$$

To complete the description of the problem, it remains to give the boundary conditions. Consistent with the linearization, the boundary conditions are imposed on a slit, for convenience taken as $y = 0$, $|x| < 1$. The limit of a quantity taken as a point approaches the top or the bottom of the airfoil is denoted by the subscript t or b. The basic condition of fluid flow, that the component of velocity normal to the body must vanish, after linearization gives

$$v_t(x) = (df_t/dx)(x) \quad (17a)$$
$$|x| < 1$$
$$v_b(x) = (df_b/dx)(x) \quad (17b)$$

where the shapes of the top and bottom of the airfoil are given by the curves $y = f_t(x)$ and $y = f_b(x)$. From the thinness and nonconductivity of the body, it may be inferred[2] that the magnetic field is continuous across the body; hence

$$\xi_t(x) = \xi_b(x) \quad (17c)$$
$$\eta_t(x) = \eta_b(x) \quad (17d)$$

moreover, from the condition that $\bar{\nabla} \times B = 0$ inside, it follows that

$$\zeta_t(x) = \zeta_b(x) = \zeta_0 \quad (17e)$$

which is an arbitrary constant.

The remaining boundary conditions depend on the nature of the solutions considered. All "elliptic" Riemann invariants are assumed to vanish at infinity, and no further restriction may be imposed. For the hyperbolic invariants, the situation depends on the orientation of the characteristics. If the characteristic does not pass through the body, then the invariant vanishes on that line. For characteristics passing through the body, the invariant vanishes on the half-line that has infinity "upstream." On the other half-line, no condition is imposed. With the subscripts 1 and 4 chosen to identify the two hyperbolic invariants of (15) and (16) and 5 and 6 to identify the two (Alfvén) invariants of (11), the remaining boundary conditions may be written, by convention, as

$$[Z_i(x)]_t = 0 \qquad i = 1,5 \qquad |x| < 1 \quad (17f)$$
$$[Z_i(x)]_b = 0 \qquad i = 4,6 \qquad |x| < 1 \quad (17g)$$

Thus the full set of boundary conditions consists of the relations (17) plus the conditions that the elliptic invariants vanish at infinity and that the hyperbolic invariants vanish if they do not intersect the body. In the next section, other relations among the boundary values are found, and the determination of the boundary values is reduced to the solution of a singular integral equation.

III. General Solution for the Hyperliptic Flow

In the hyperliptic regime, the characteristic equation (8) has one pair of complex conjugate roots, $\lambda_2 = s + it$ and $\lambda_3 = \bar{\lambda}_2$. If the complex variable

$$z = X + iY = x + sy + ity \quad (18)$$

is introduced, (7) becomes

$$(\partial/\partial\bar{z})Z_2 = 0 \quad (19)$$

Hence, Z_2 is an analytic function of z. The relation between the (x,y) and (X,Y) planes is a simple affine transformation that reduces to the identity on the x axis.

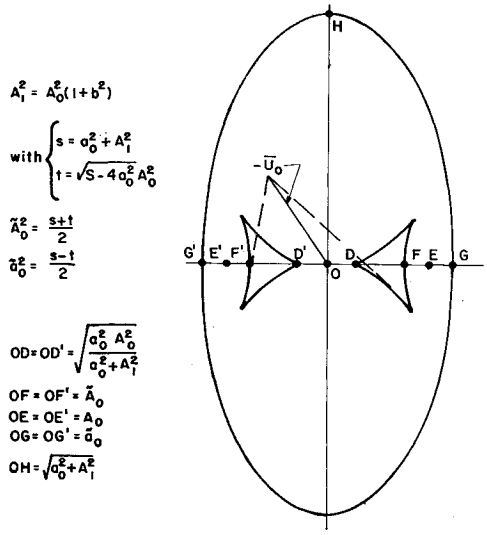

Fig. 1 Section of the ray cone for a two-dimensional magnetohydrodynamic wave

The function Z_2 may be expressed in terms of its real and imaginary parts as $Z_2 = W_1 + iW_2$. Since Z_2 is an analytic function of $z = X + iY$, it may be represented as a Cauchy integral in terms of its boundary values. Under the assumption that Z_2 tends to zero at infinity sufficiently rapidly, this representation has the form

$$Z_2 = \frac{1}{\pi i}\int_{-1}^{1} \frac{F(\rho) + iG(\rho)}{\rho - z}\, d\rho \quad (20)$$

Thus, Z_2 must go to zero at infinity at least as fast as z^{-1}.

By the well-known Plemelj formulas, the boundary values of W_1, W_2 are determined from (20) as

$$[W_1(x)]_t = F(x) + \frac{1}{\pi}\int_{-1}^{1} \frac{G(\rho)}{\rho - X}\, d\rho \quad (21a)$$

$$[W_1(x)]_b = -F(x) + \frac{1}{\pi}\int_{-1}^{1} \frac{G(\rho)}{\rho - X}\, d\rho \quad (21b)$$

$$[W_2(x)]_t = G(x) - \frac{1}{\pi}\int_{-1}^{1} \frac{F(\rho)}{\rho - X}\, d\rho \quad (21c)$$

$$[W_2(x)]_b = -G(x) - \frac{1}{\pi}\int_{-1}^{1} \frac{F(\rho)}{\rho - X}\, d\rho \quad (21d)$$

where the integrals are defined as Cauchy principal values. Alternate forms for (21a) or (21b) and for (20c) or (20d) are obtained by elimination from (21):

$$[W_1(x)]_t - [W_1(x)]_b = 2F(x) \quad (21a')$$

$$[W_2(x)]_t - [W_2(x)]_b = 2G(x) \quad (21c')$$

With Eqs. (21), the reduction of the problem to relations amoung boundary values is completed. From (17a) and (17b), it follows that $v_t(x)$ and $v_b(x)$ are known functions. Since the magnetic field is continuous [(17c) and (17d)], there are only two unknown functions relating to the boundary values of the magnetic field: $\xi(x)[= \xi(x)_t = \xi(x)_b]$ and $\eta(x)[= \eta(x)_t = \eta(x)_b]$. The constant $\zeta_0[= \zeta_t(x) = \zeta_b(x)]$ remains arbitrary. Thus the system of Eqs. (17f, 17g, 21a', and 21c') is a system of six linear equations in the eight unknowns $\sigma_t(x)$, $\sigma_b(x)$, $\xi(x)$, $\eta(x)$, $w_t(x)$, $w_b(x)$, $F(x)$, and $G(x)$. The inhomogeneous terms in the system are linear combinations of $v_t(x)$, $v_b(x)$, and ζ_0. Thus, σ_t, σ_b, ξ, η, w_t, w_b may be expressed as linear combinations of $F(x)$, $G(x)$, and the known functions v_t, v_b, and ζ_0. Hence $W_1(x)$ and $W_2(x)$ on the top or bottom of the airfoil are also linear combinations of the same

functions. The two integral relations (21b) and (21d) then become integral equations of the form

$$AH + \frac{1}{\pi} B \int_{-1}^{1} \frac{H(\rho)}{\rho - x}\, d\rho = C \tag{22}$$

where A and B are two-by-two matrices with constant coefficients, C is a two-component vector whose components are known linear combinations of $v_i(x)$, $v_b(x)$, and ζ_0, and H represents the two-component vector (F,G). The matrix A is assumed to be nonsingular, and premultiplication of (22) by A^{-1} gives

$$H + \frac{1}{\pi} B' \int_{-1}^{1} \frac{H(\rho)}{\rho - x}\, d\rho = C' \tag{23}$$

Equation (23) is the desired integral equation for the boundary values. The solution is given below.

There exists a nonsingular matrix Q such that $\hat{B} = QB'Q^{-1}$ is in subdiagonal form

$$\hat{B} = \begin{pmatrix} \mu & 0 \\ a & \nu \end{pmatrix} \tag{24}$$

where $a \neq 0$ only if $\mu = \nu$. Under the transformation $\hat{H} = QH$, Eq. (23) becomes

$$\hat{H} + \frac{1}{\pi} \hat{B} \int_{-1}^{1} \frac{\hat{H}(\rho)}{\rho - x}\, d\rho = QC' \tag{25}$$

which represents the pair of inhomogeneous singular integral equations with a Cauchy-type kernel

$$\hat{H}_1 + \frac{\mu}{\pi} \int_{-1}^{1} \frac{\hat{H}_1(\rho)}{\rho - x}\, d\rho = (QC')_1 \tag{26a}$$

$$\hat{H}_2 + \frac{\nu}{\pi} \int_{-1}^{1} \frac{\hat{H}_2(\rho)}{\rho - x}\, d\rho = (QC')_2 - \frac{a}{\pi} \times \int_{-1}^{1} \frac{\hat{H}_1(\rho)}{\rho - x}\, d\rho \tag{26b}$$

Provided $\mu^2, \nu^2 \neq -1$, Eq. (26a) is solved for $\hat{H}_1$ by standard techniques (see, for instance, Mikhlin[4]), and the solution is substituted in the right-hand side of (26b), which is then solved for $\hat{H}_2$.

The solution of an integral equation of the type

$$\phi(x) + \frac{\delta}{\pi} \int_{-1}^{1} \frac{\phi(\rho)}{-x}\, d\rho = f(x) \tag{27}$$

is given by

$$\phi(x) = \frac{1}{1 + \delta^2} f(x) - \frac{1}{\pi} \frac{\delta}{1 + \delta^2} (1 + x)^{m-1} \times (1 - x)^{-m} \int_{-1}^{1} (1 + \rho)^{1-m}(1 - \rho)^{m} f(\rho)(\rho - x)^{-1} d\rho + K(1 + x)^{m-1}(1 - x)^{m} \tag{28}$$

where m is determined from

$$e^{2\pi i m} = (1 + i\delta)/(1 - i\delta) \qquad 0 \leq Re(m) < 1 \tag{29}$$

and K is an arbitrary constant. If $f(x)$ is well behaved, e.g., $f(x)$ has a Lipshitz continuous derivative, then it may be shown easily that

$$\phi(x) = \frac{1}{2^{1-m}} \cdot \frac{(C + K)}{(1 - x)^{m}} + O[(1 - x)^{1-m}] \quad \begin{matrix} x \to 1 \\ x < 1 \end{matrix} \tag{30a}$$

$$\phi(x) = \frac{1}{2^{m}} \cdot \frac{(C' + K)}{(1 + x)^{1-m}} + O[(1 + x)^{m}] \quad \begin{matrix} x \to 1 \\ x > -1 \end{matrix} \tag{30b}$$

where

$$C = \frac{\delta}{\pi(1 + \delta^2)} \int_{-1}^{1} d\rho\, f(\rho) \left(\frac{1 + \rho}{1 - \rho}\right)^{1-m} \tag{31a}$$

$$C' = -\frac{\delta}{\pi(1 + \delta^2)} \int_{-1}^{1} d\rho\, f(\rho) \left(\frac{1 - \rho}{1 + \rho}\right)^{m} \tag{31b}$$

Hence K may be chosen so that $\phi(x)$ is regular (and even vanishes) at the leading edge or at the trailing edge. However, $\phi(x)$ will be singular at one edge or the other unless f is chosen specially. Such a choice of f implies a special shaping of the body, as is considered briefly below.

With the solutions to the integral equations of the form (26), it remains to describe the solution of the original problem. $\hat{H}_1(x)$ and $\hat{H}_2(x)$, linear combinations of $F(x)$ and $G(x)$, satisfied (26); thus $\hat{H}_1(x)$ and $\hat{H}_2(x)$ may be written in the form (28) with constants m_1, K_1 and m_2, K_2. Furthermore, near the ends of the body, $\hat{H}_1(x)$ and $\hat{H}_2(x)$ have the behavior given in (30) with the appropriate m and K. It follows that $F(x)$ and $G(x)$ are each the sum of two expressions of the form (28) with constants m_1, K_1 and m_2, K_2. Since $Z_2(z)$ is given by (20), it easily is seen that for z near the leading or trailing edge, i.e, $y \to 0$, $x \to \pm 1$,

$$Z_2(z) = \frac{\alpha}{(1 - z)^{m_1}} + \frac{\beta}{(1 - z)^{m_2}} + O(1) \quad z \to +1 \tag{32a}$$

$$Z_2(z) = \frac{\alpha'}{(1 + z)^{1-m_1}} + \frac{\beta'}{(1 + z)^{1-m_2}} + O(1)\ z \to -1 \tag{32b}$$

Again, with judicious choice of the two constants K_1 and K_2, one constant of each pair of constants (α,α') and (β,β') may be set to zero.

Now that the elliptic part of the solution has been completed, the hyperbolic part also must be given. Since $F(x)$ and $G(x)$ are known, Eqs. (17) and (20) constitute six equations for the six unknowns σ_t, σ_b, ξ, η, w_t, and w_b. Thus these variables are given as a linear combination of $F(x)$, $G(x)$, and the known functions $v_t(x)$, $v_b(x)$, and ζ_0. The Riemann invariants previously unspecified on the body have the form

$$[Z_i(x)]_b = \alpha_i F(x) + \beta_i G(x) + R_i(x) \qquad |x| < 1 \qquad i = 1,5 \tag{33a}$$

$$[Z_i(x)]_t = \alpha_i F(x) + \beta_i G(x) + R_i(x) \qquad |x| < 1 \qquad i = 4,6 \tag{33b}$$

where $R_i(x)$ are well-behaved functions of x. Since the ith Riemann invariant is constant on the line $x + y\lambda_i$, the nonzero values of the Riemann invariants are given everywhere by (33) on the replacement $x \to x + y\lambda_i$. Hence the singularities present in $F(x)$ and $G(x)$ at the tips of the body propagate along characteristics. In general, the real Riemann invariants behave like

$$Z_i(x,y) = \frac{\gamma}{(1 - x - y\lambda_i)^{m_1}} + \frac{\gamma''}{(1 - x - y\lambda_i)^{m_2}} + O(1) \quad \begin{matrix} x + y\lambda_i \to 1 \\ x + y\lambda_i < 1 \end{matrix} \tag{34a}$$

$$Z_i(x, y) = \frac{\gamma'}{(1 + x + y\lambda_i)^{1-m_1}} + \frac{\gamma'''}{(1 + x + y\lambda_i)^{1-m_2}} + O(1) \quad (34b)$$

$$x + y\lambda_i \to -1$$
$$x + y\lambda_i > -1$$

The choice of K_1 and K_2 which removed a singularity of a complex invariant eliminates the corresponding singularities in the real invariants. The value of any Riemann invariant on its characteristic is zero unless the characteristic ends on the body, and then its value is given by (17f, 17g, or 33). Since each physical variable is a linear combination of all the Riemann invariants, each variable has the composite behavior implied by (32) and (34). Hence, as one approaches a characteristic through a tip, the behavior anywhere in the fluid is given by (34). As one approaches a tip itself, the behavior is the sum of terms from (32) and (34).

An expression of the form $1/|1 - x - y\lambda|^m$, occurring in (34), is square integrable on line segments or over areas only if $m < \frac{1}{2}$. Hence, the singularities in (34a) and (34b) from a given exponent are not both square integrable. The singularities in the complex invariant [see (32)] are square integrable over areas provided $0 < m < 1$. The generalized Kutta-Joukowsky condition of the next section is based on these observations.

In the case $b = 0$, the variables ζ and w separate out, and the Riemann invariants Z_5 and Z_6 may be ignored or considered separately. Now it is possible to obtain directly from (21a′) and (21c′) a linear relation between $F(x)$, $G(x)$, and known functions. Hence there is only one integral equation and one exponent m and constant K. Otherwise there are no changes from the foregoing description. In a loose sense, the second singularity is associated with the other variables.

IV. A Generalized Kutta-Joukowsky Condition

The present section deals with the choice of the constants K_1, K_2 necessary for a unique solution. In ordinary fluid dynamics, a similar nonuniqueness occurs in the subsonic solution; in this case a single integral equation is solved, $m = \frac{1}{2}$, and the solution contains one arbitrary constant. The Kutta-Joukowsky condition requires smooth flow at a sharp trailing edge and is equivalent to the addition of sufficient circulation of the flow to cause a confluence of the rear stagnation point on the body with the trailing edge. The singularity at the leading edge remains in the linearized solution, in general, unless the body is shaped to remove it.

In the magnetofluiddynamic case, the singularities in the physical variables have exponents m_i and $1 - m_i$ ($i = 1, 2$, $0 < m_i < 1$) at the trailing and leading edges, respectively. In the restricted problem there is only one exponent m corresponding to singularities of order m and $1 - m$ at the trailing and leading edges. The proposed condition is to require the square integrability of these variables over any finite region in the flow, in particular, in the neighborhood of the line singularities. This condition uniquely specifies the two constants K_i and K_2 [see (30) and (31)]. In an exact solution, such square integrals must exist, as they represent the energy in a region or the forces acting there. If the proposed condition were not valid, then the linearized solution would be a bad approximation to the exact solution near the line singularities both pointwise and in the square-integral sense. Thus, nonlinear or dissipative phenomena would affect the gross characteristics of the flow, and the linearized solution would have almost no meaning. Hence, if the linearized solution is to be taken as a valid approximation (except in certain regions), then it must be used in conjunction with the proposed condition. The weaker point and line singularities remaining in the flow are not expected to be good pointwise approximations to the correct flow there, and a nonlinear, dissipative analysis may have to be done to improve the solution in these regions. Nonetheless, one might hope that the overall characteristics of the linearized solution are reasonably correct, as in ordinary fluid dynamics, where integral properties such as lift on the airfoil are predicted fairly accurately by the linearized theory. However, experimental results will be the final arbiter.

For the restricted problem, a curve in the hyperliptic region was found which separates regions $m > \frac{1}{2}$ from $m < \frac{1}{2}$. On the two sides of this critical curve, m has the values 1 and 0. It is instructive to follow the behavior of the singularities as the critical curve is crossed, say, from a region $m < \frac{1}{2}$ to a region $m > \frac{1}{2}$ (e.g., by varying $\bar{U}_0$). In the region $m < \frac{1}{2}$, the leading edge singularity is removed. As the critical curve is approached, the trailing edge singularity tends to zero, and at the critical curve there is no singularity at either edge. On entering the region $m > \frac{1}{2}$, m is close to unity, the trailing edge singularity is removed, and the leading edge singularity is small. The total effect of crossing the critical curve is that the singularity disappears from one edge and reappears at the other. It is noted that this is a continuous process and is dependent on the Kutta condition used. If, say, a condition that the trailing edge singularity be removed were used instead, then there would be a discontinuous disappearance of the singularity at the leading edge across the critical curve.

A Kutta condition having similar effect to the one just described has been obtained by Stewartson[5] for the restricted problem in the incompressible limit. The removal of one of the edge singularities in either region $m > \frac{1}{2}$ or $m < \frac{1}{2}$ is related to its removal on the relevant side of the critical curve. There, the singularity at one of the edges has the limit unity for its exponent, and when $m = 0$ (or 1) there are infinite forces on the body in the neighborhood of the leading (or trailing) edge. Since such a solution is unacceptable, Stewartson, by a continuity argument, removes that singularity whose exponent tends to one as the critical curve is approached from the relevant side. Thus Stewartson's condition produces the same result as the one proposed here, but it is imposed for different reasons. The argument here is based on the unacceptability of the solution without the proposed Kutta-Joukowsky condition without recourse to any continuity arguments. The distinction is clear in the general two-dimensional case where Stewartson's criterion is inapplicable, as computations have shown that the two exponents m_1 and m_2 never become zero or one.

In the preceding discussion, the thin blunt body has been omitted. If the functions $f_t(x)$ and $f_b(x)$ are to correspond to a blunt body, then they may be taken of the form

$$f_{t,b}(x) = c_{t,b}(1 - x)^r + (1 - x)g_{t,b}(x) \quad \text{as } x \to 1 \qquad 0 < r < 1$$

or

$$f_{t,b}(x) = d_{t,b}(1 + x)^{r'} + (1 + x)h_{t,b}(x) \quad \text{as } x \to -1 \qquad 0 < r' < 1$$

where $g_{t,b}$ and $h_{t,b}$ are regular. Since $v_t(x)$ and $v_b(x)$, which are given by (17a) and (17b), appear in the inhomogeneous terms of the integral equation (27), these terms of the integral equation have the behavior [see (27)]

$$f(x) = c'(1 - x)^{r-1} + 0(1) \qquad \text{as } x \to 1$$

and

$$f(x) = d'(1 + x)^{r'-1} + 0(1) \quad \text{as } x \to -1$$

Hence the estimates (30) et seq. no longer apply. Nonetheless, (28) is still the solution to the integral equation (27), and the properties of the solution may be inferred readily from (27). Since $f(x)$ appears explicitly in (28), the solution should have at least the singularities present in $f(x)$. Besides these terms, there also will be the singularities of Eqs. (30) et seq.

The stronger of the singularities of the type of (30) may be removed as before, but the new singularities introduced by

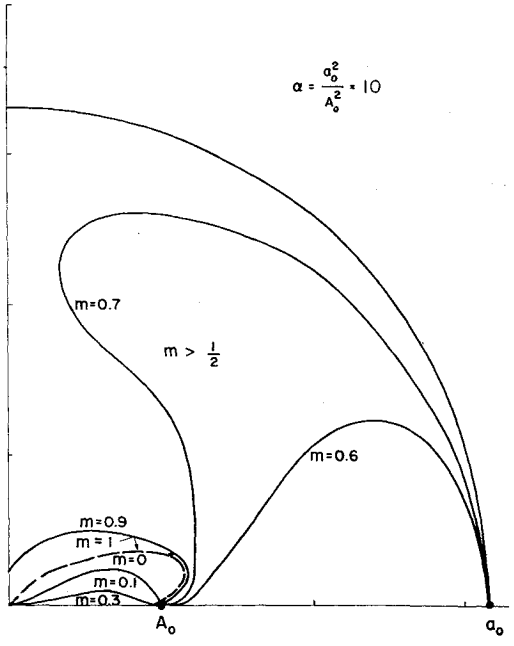

Fig. 2 Exponents m of singularities for $\alpha = 10$

the blunt ends persist. They are acceptable, according to the proposed Kutta-Joukowsky condition, only if $r' > \frac{1}{2}$ so that the possible relevance of the linearized solution is restricted to these cases.

V. Classification of the Singularities

The exponents m_i of the singular terms involved in the solution of the integral equations (26) are complicated functions of the unperturbed velocity and magnetic fields $\bar{U}_0$, $\bar{B}_0$ and the Alfven and sound speeds A_0, a_0. Numerical calculations were performed to investigate the variation of m with these parameters.

In the restricted two-dimensional problem, m has a single value that may be obtained directly from the coefficient δ of the integral equation corresponding to (27) for F or G (recall that F and G are related). The formulas necessary for this calculation are set out in Appendix B. Computations were made to find m in the hyperliptic region (that is, over the whole range of values of U_0 and θ) for a range of values of the ratio $\alpha = a_0^2/A_0^2$. When the coefficient δ is positive, $m = 1/\pi \tan^{-1}\delta$, and $0 < m < \frac{1}{2}$. When δ is negative, $m = 1 + 1/\pi \tan^{-1}\delta$, and $\frac{1}{2} < m < 1$. Hence, where δ changes sign, m jumps from zero to unity; this curve separates regions of $m < \frac{1}{2}$ from $m > \frac{1}{2}$ and is called the critical curve.

Figures 2–7 indicate the variation of the critical curve in the restricted problem over the range of values of α, and various contour lines of m are shown also. The figures represent one quadrant of the hyperliptic region, and the complete diagram can be obtained by reflection in the axes. The unperturbed magnetic field $\bar{B}_0$ is taken along the horizontal axis (as in Fig. 1). The velocity vector $\bar{U}_0$ extends from the origin, and the size and inclination of this vector with respect to the other parameters then determine m and on which side of the critical curve it lies. Flows with $\bar{U}_0$ and $\bar{B}_0$ perpendicular always lie in the region $m > \frac{1}{2}$. For large α, the critical curve is a continuous curve from the origin to the cusp on the axis of the inner wave front. The region $m < \frac{1}{2}$ increases in area as α decreases and splits into two branches as it overlaps with the outer limit of the hyperliptic region (Fig. 4). The branch to the inner wave front is lost as the limit $a_0^2 = A_0^2$ is passed, and for $\alpha < 1$ the critical curve extends from the origin to the point $(a_0^2 + A_0^2)^{1/2}$ on the perpendicular to $\bar{B}_0$. Figure 2, corresponding to the incompressible limit (A_0 fixed, $a_0 \to \infty$), shows Stewartson's result that the critical curve is given by

$$M_0^2 = \cos 2\theta \tag{35}$$

Alternatively, it represents the limit of vanishing magnetic field ($A_0 \to 0$, a_0 fixed), in which case the $m < \frac{1}{2}$ region is very small and the Kutta-Joukowsky condition of ordinary fluid dynamics is recovered as a limit of the generalized uniqueness condition.

The results just obtained may be checked with information inferred from certain expansions of δ, which is related to m by (29). For small values of U_0, the coefficient δ of the integral equation in the restricted case has the behavior

$$\delta \sim \alpha m_0 \cos 2\theta / \{\sin\theta (1 + \alpha)^{1/2}\} \tag{36}$$

Thus the critical curve has slope $\pi/4$ at the origin. In the

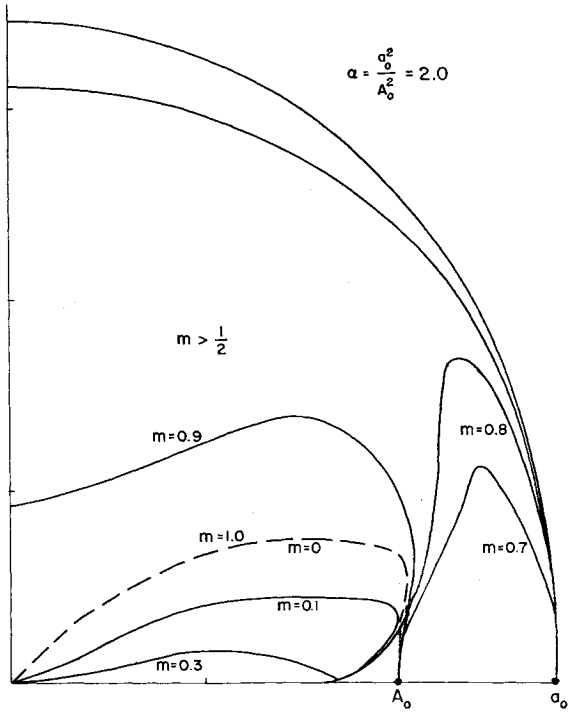

Fig. 3 Exponents m of singularities for $\alpha = 2.0$

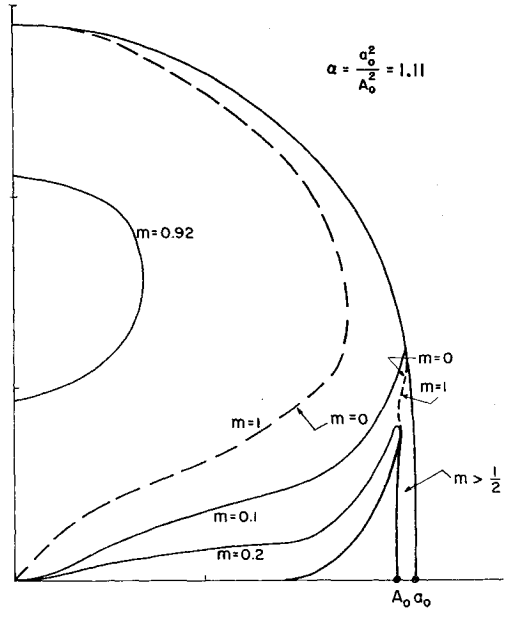

Fig. 4 Exponents m of singularities for $\alpha = 1.11$

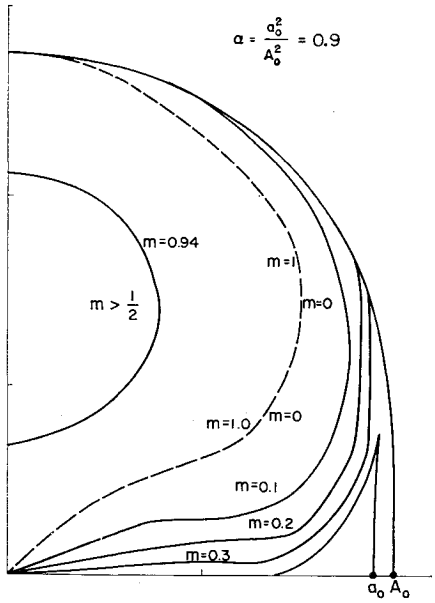

Fig. 5 Exponents m for singularities $\alpha = 0.9$

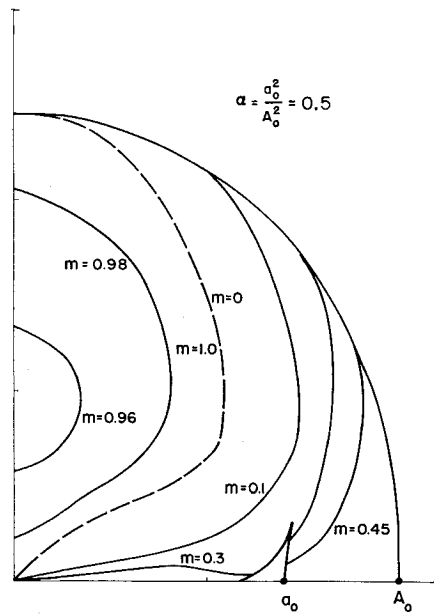

Fig. 6 Exponents m of singularities for $\alpha = 0.5$

limit $\theta \to 0$, U_0 arbitrary but fixed,

$$\delta \sim 2\alpha m_0(1 - m_0^2)\left(\frac{1}{1+\alpha} - m_0^2\right) \Big/ \{\theta C (1+\alpha)^{1/2} \times [\alpha^2 m_0^2 + (1+\alpha)(1-m_0^2)^2]\} \quad (37)$$

where

$$C = \{(1 - m_0^2)(1 - M_0^2)/(1 - m_0^2 - m_0^2)\}^{1/2} \quad (38)$$

Hence δ changes sign twice, once at $U_0 = a_0$ and once at $U_0 = a_0 A_0/(a_0^2 + A_0^2)^{1/2}$, the latter point being the position of the cusp of the inner wave front on the $\bar{B}_0$ axis. For $\alpha > 1$ (so that the velocity vector $U_0 = a_0$, $\theta = 0$ lies on the outer wave front), δ has opposite signs in the hyperliptic region on the different sides of the cusp (near $\theta = 0$), and δ vanishes at the cusp. As was observed in Figs. 2–4, the critical curve leaves the origin and re-enters the cusp. For $\alpha < 1$ (so that the vector velocity $U_0 = a_0$, $\theta = 0$ lies on the inner wave front), δ has only one sign near $\theta = 0$ in the hyperliptic region. Now the critical curve leaves the origin and terminates at $U_0 = (a_0^2 + A_0^2)^{1/2}$, $\theta = \pi/2$. Sears and Grad have shown that when $\bar{U}_0$ and $\bar{B}_0$ are parallel the system behaves as an ordinary fluid, whereas from (36), as $\theta \to 0$, $m \to +\frac{1}{2}$, the fluid dynamic result. Without much more care, little more can be inferred from this treatment of the parallel flow case.

Numerical calculations to determine the exponents m_1, m_2 in the general two-dimensional case also were performed. The equations leading to the coupled integral equation (20) are given in Appendix C. The numerical results indicate $0 \leq m_1 < \frac{1}{2} < m_2 \leq 1$, where $m_i \to \frac{1}{2}$ as $\theta \to 0$.

According to the proposed uniqueness condition, there is a singularity of exponent m_1 at the leading edge and a singularity of exponent $1 - m_2$ at the trailing edge. Thus the leading edge singularity is stronger or weaker than the one at trailing edge as $m_1 + m_2$ is greater or less than 1. In Figs. 8–14, the curves $m_1 + m_2 = 1$ are exhibited for various values of the parameters. The unit of speed is the Alfven speed A_0. For b large, the two branches of the critical curve do not fit conveniently on one scale; hence part of Figs. 11, 13, and 14 is shown in a reduced scale on the left. In such cases the second branch is suppressed in the right-hand figure. The inner wave front either is drawn, or, if it is too small, its position is indicated by a square. In each figure, one region is marked for which $m_1 + m_2$ is greater or less than one. In all cases, as the curves are crossed, the inequality changes.

For small values of b, one exponent should be close to the one computed when $b = 0$, and the other should be near zero or one. Hence the curve on which $m = 0$ (or 1) for $b = 0$ should approximate the curve $m_1 + m_2 = 1$ for $b \neq 0$ but small. Thus Figs. 8 and 12 are similar to Figs. 6 and 3, respectively. However, in each case there is one additional curve when $b \neq 0$, but this curve vanishes as b goes to zero. Hence the distinctions present between $\alpha > 1$ and $\alpha < 1$ when $b = 0$ also occur for small values of $b \neq 0$. As shown in Figs. 9–11, as b increases the nature of the curves changes for $\alpha < 1$, so that the distinctions between $\alpha < 1$ and $\alpha > 1$ disappear.

Because of various difficulties in the numerical work, certain features of Figs. 8–14 cannot be verified readily. First, it is not definitely known that the curves enter the origin as shown. Second, it is not clear that the curves shown to intersect the outer surface of the ray cone do not continue very close to the cone and end at some other place. In both cases the numerical work strongly indicates the conclusions implied by the figures.

For large b, and m_0 and M_0 fixed, the coefficients μ,ν of the integral equation (26) are given by

$$\mu \sim \frac{M_0(\cos 2\theta - M_0^2)}{\sin\theta(1 + M_0^2)} + O\left(\frac{1}{b}\right) \quad (39a)$$

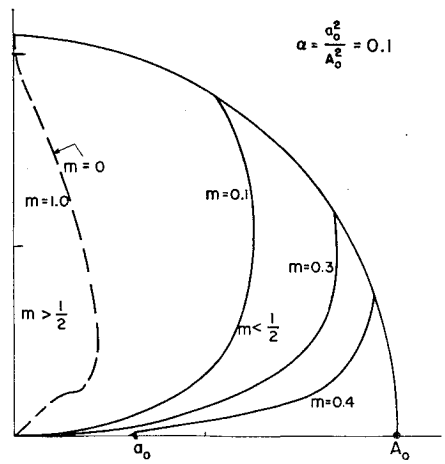

Fig. 7 Exponents m of singularities for $\alpha = 0.1$

$$\nu \sim \frac{-m_0 M_0^2 \sin\theta}{b(\cos 2\theta - M_0^2)} + O\left(\frac{1}{b^2}\right) \tag{39b}$$

An alternate description of the critical curve would be a curve across which $\mu + \nu$ changes sign. From (39a) and (39b), one branch of the curve for b large is seen to be

$$M_0^2 = \cos 2\theta \tag{40}$$

The other branch, found by setting m_0^2 and $M_0^2 = O(b^2)$, was computed to be

$$M_0^2 + m_0^2 \sin^2\theta = b^2 \tag{41a}$$

or, with $M_0^2 = \alpha m_0^2$,

$$M_0^2 = \alpha b^2/(\alpha + \sin^2\theta) \tag{41b}$$

For m_0^2 and $M_0^2 = O(b^2)$, the coefficients μ and ν of the integral equation (26) were found to be

$$u \sim \frac{m_0 \sin\theta}{(b^2 - M_0^2)^{1/2}} = \frac{m_0 \sin\theta}{(b^2 - \alpha m_0^2)^{1/2}} \tag{42a}$$

$$\nu \sim \frac{(b^2 - M_0^2)^{1/2}}{m_0 \sin\theta} = \frac{(b^2 - \alpha m_0^2)^{1/2}}{m_0 \sin\theta} \tag{42b}$$

where $M_0^2/b^2 = \alpha m_0^2/b^2 < 1$ is necessary if the velocity U_0

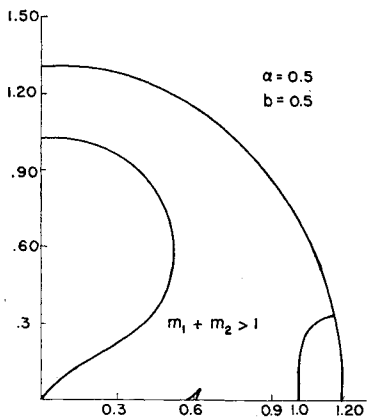

Fig. 8 Critical curves for $\alpha = 0.5$, $b = 0.5$

is to remain in the hyperliptic region for large b. Without further terms in the expansion (41), it is not possible to decide whether or not this branch of the critical curve intersects the characteristic cone for large b.

VI. Flow Near Singular Edges

In order to understand the nature of the singularities present in this problem, the flow quantities in the neighborhood of the leading and trailing edges have been computed numerically. Various surprising features of the flow appear, the interpretation of which is obscure. The flows also are exhibited for singularities rejected by the proposed uniqueness condition. The flows suppressed by the uniqueness condition are marked accordingly. To facilitate computation, only the restricted strictly two-dimensional problem was considered. It suffices to consider the solutions to the homogeneous integral equations, i.e., functions representing flow past a flat

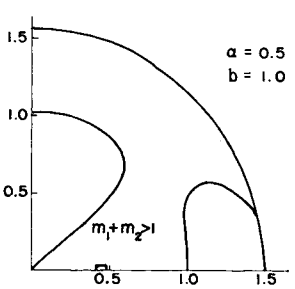

Fig. 9 Critical curves for $\alpha = 0.5$, $b = 1.0$

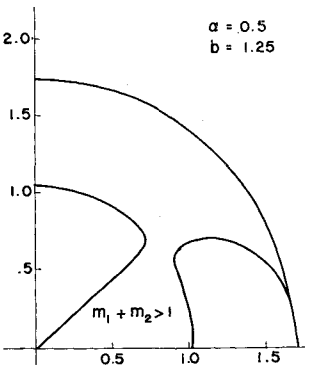

Fig. 10 Critical curves for $\alpha = 0.5$, $b = 1.25$

body, since these solutions possess the same singularities as do solutions of the inhomogeneous problem. The leading and trailing edges may be treated separately, so that the body becomes the positive or the negative real axis with the origin at the leading or the trailing edge, respectively. Under these assumptions, the flow becomes a similarity flow; the flow direction is the same at all points along a ray from the origin. A series of flows was computed numerically for a range of values of the parameters both in the $m > \frac{1}{2}$ and $m < \frac{1}{2}$ regions. Figures 15–18 show the shape of the streamlines of these flows near the leading and trailing edges. The characteristics through the edge are indicated as well as asymptotes of the flow when they occur.

The point singularity is taken in the form

$$Z_2 = W_1 + iW_2 = (1 + i\gamma)Z^{-n} \tag{43}$$

where $n = 1 - m$ or m at a leading or trailing edge. The coefficient γ is determined in terms of the discontinuities across the body in W_1 and W_2. The complete details of the derivation of the flows computed in this section are given in Appendix D. The right-hand side of (43) may be multiplied by a real constant, thus affecting the flow variable but not affecting the ratio v/u. Hence the streamline shape is invariant. The only question outstanding is the positive or negative direction of the flow along the streamlines. Figures 15–18 therefore must be regarded as one of two possible flows, the second being the reversal of the one shown.

The flow quantities have infinite values along the characteristics from the leading and trailing edges, but the ratio v/u remains finite as these characteristics are approached. However, there is a discontinuous change in the streamline shape at the characteristic. In fact, it can be seen from the diagrams that these singular characteristics in a sense may act as line source or sinks. That is, although the solutions do solve the linearized equations in a generalized sense, the linearized equations are a bad approximation to the nonlinear ones in the neighborhood of the characteristics. Thus, the linearized equations represents there a bad approximation to mass conservation. It is to be noted that the strength of the line

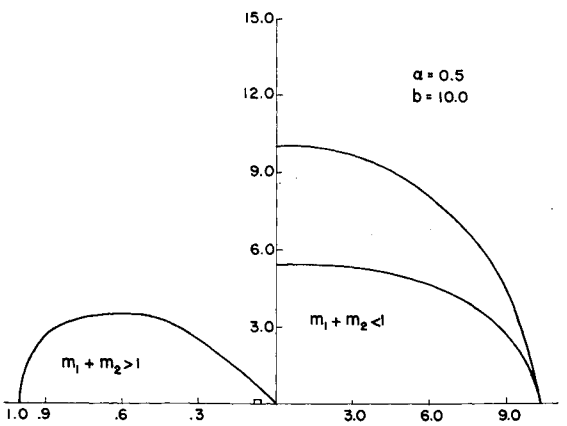

Fig. 11 Critical curves for $\alpha = 0.5$, $b = 10.0$

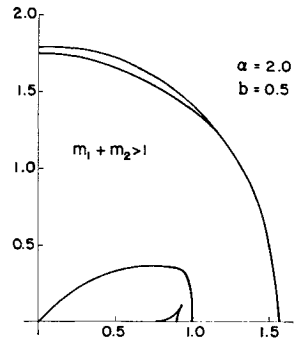

Fig. 12 Critical curves for $\alpha = 2.0$, $b = 0.5$

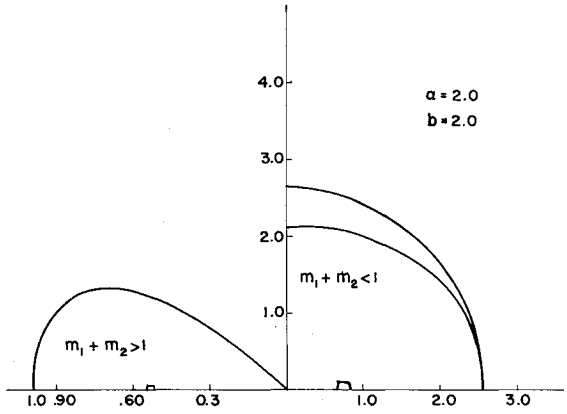

Fig. 13 Critical curves for $\alpha = 2.0$, $b = 2.0$

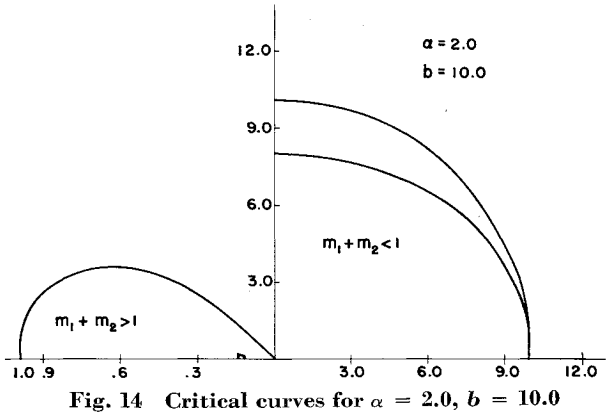

Fig. 14 Critical curves for $\alpha = 2.0$, $b = 10.0$

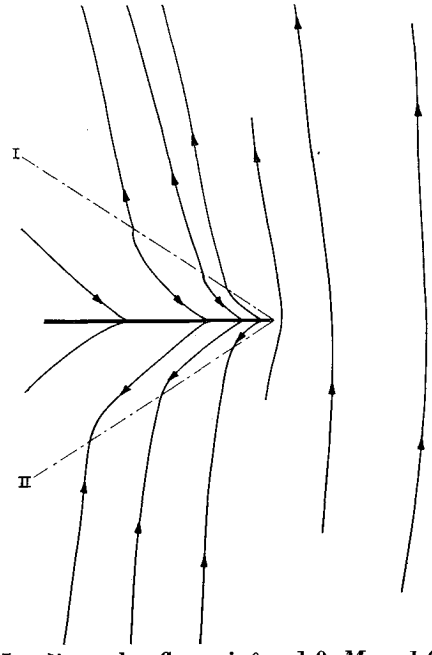

Fig. 15 Leading-edge flow, $\sin\theta = 1.0$, $M_0 = 1.0$, $\alpha = 0.5$, $1 - m = 0.022584$

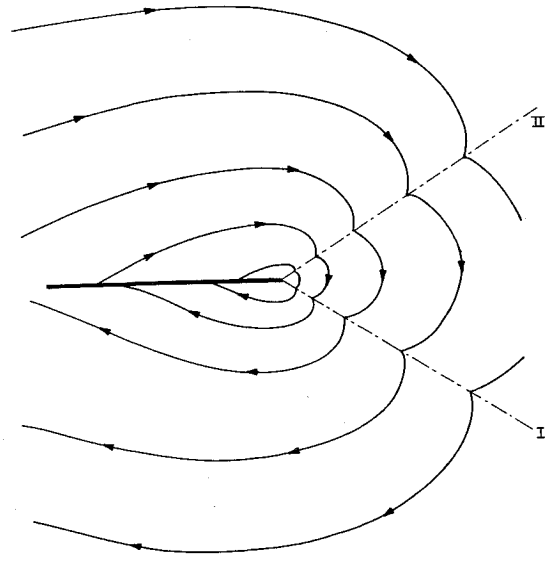

Fig. 16 Trailing-edge flow, $\sin\theta = 1.0$, $M_0 = 1.0$, $\alpha = 0.5$, $m = 0.977416$, flow suppressed

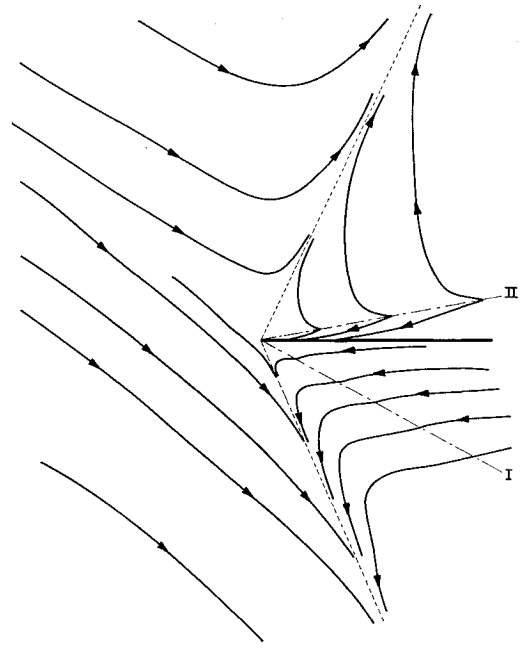

Fig. 17 Leading-edge flow, $\sin\theta = 0.45$, $M_0 = 0.95$, $\alpha = 0.5$, $1 - m = 0.62326$, flow suppressed

singularity is undiminished at large distances from the body. It is possible that the introduction of shocks emanating from the leading and trailing edges may be needed. The regional effect of the line singularities of the linearized solution may provide a first approximation to the shock solution. It should be noted that even with the proposed Kutta condition the flows have many surprising features that require further investigation and explanation. One unfortunate possibility that should not be overlooked is that ordinary linear theory does not provide meaningful answers for this problem.

The flow diagrams may be interpreted as the hyperbolic flow carried along the characteristic superposed on the flow in the whole region near an edge due to the elliptic point singularity. The flow in the domain of dependence near an edge characteristic is dominated by the hyperbolic flow, but this influence weakens away from these characteristics. At points where the two constituent flows are opposing, asymptotes develop. The effect of the point singularity outside the domain of dependence is evident as a mixture of a circulatory flow around an edge and a flow developing asymptotes.

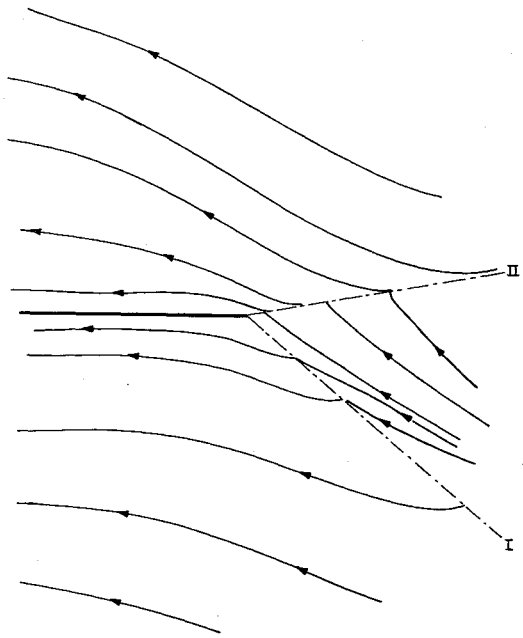

Fig. 18 Trailing-edge flow, $\sin\theta = 0.45$, $M_0 = 0.95$, $\alpha = 0.5$, $m = 0.37674$

Appendix A

Specific solutions for flow quantities in the $\theta = \pi/2$ case are given. In this case it is seen easily from the symmetry properties of the differential equation and boundary condition that if the body is antisymmetric [i.e., $f_t(x) = f_b(x)$], and if $(\sigma,v,w,\xi,\eta,\zeta)(x,y)$ is a solution of the boundary value problem, then $(-\sigma,v,w,\xi,-\eta,-\zeta)$ $(x,-y)$ is also a solution. Hence v,w, and ξ are even functions of y, and σ,η, and ζ are odd in y. Similarly, if $f_t(x) = -f_b(x)$, v,w, and ξ are odd in y, and σ,η,ζ are even in y. It is evident that, in general, the solution can be represented as the sum of two solutions, one depending only on the even part, $\frac{1}{2}[(v)_t + (v)_b]$, of the assigned values of v, and the other only on the odd part, $\frac{1}{2}[(v)_t - (v)_b]$. This decomposition corresponds to the diagonalization of the system (22).

An explicit representation for boundary values of the solution is given explicitly. It is supposed that the boundary values of v are decomposed as a sum

$$(v)_t = g + k \tag{A1}$$

$$(v)_b = g - k \tag{A2}$$

The solution is a sum of two functions. One, depending on g alone, represents the flow about a body with no thickness (cambered body); the other, depending on k alone, represents the flow about a symmetric body.

In the first case (cambered body), solution for boundary values of the density σ is given by

$$(\sigma)_t = -(\sigma)_f = \frac{m_0^2}{\mu^2+\nu^2}\left\{\mu g(x) - \frac{\nu}{\pi}(1+x)^{m-1}\times (1-x)^{-m}\int_{-1}^{1}(1+s)^{1-m}(1-s)^m \times (s-x)^{-1}g(s)ds\right\} + c(1+x)^{m-1}(1-x)^{-m} \tag{A3}$$

where

$$m = m_2 = 1 + (1/\pi)\tan^{-1}(\nu/\mu) \qquad (\tfrac{1}{2} \le m_2 < 1) \tag{A4}$$

$$\mu = \lambda_1(1+\lambda_1^2 - M_0^2)(1+b^2-b^2t^2)(\lambda_1^2+t^2)^{-1}\times (1+b^2+b^2M_0^2)^{-1} + M_0b^2(1+b^2+b^2M_0^2)^{-1} \tag{A5a}$$

$$\nu = -t(1+b^2+b^2\lambda_1^2)(t^2+M_0^2-1)(\lambda_1^2+t^2)^{-1}\times (1+b^2+b^2M_0^2)^{-1} \tag{A5b}$$

and λ_1, $-\lambda_1$, it, $-it$ are the characteristic roots of the linearized flow equations.

Since $m_2 > \frac{1}{2}$, the uniqueness condition is applied at the trailing edge. The pressure difference across the body is given by

$$(p)_t - (p)_b = 2\rho_0 u_0^2[(\sigma)_t/m_0^2] \tag{A6}$$

The solution (A3) in the case $b = 0$ with a Kutta condition applied at the trailing edge corresponds to the solution obtained by McCune using a Prandtl-Glauert transformation in conjunction with the incompressible theory of Sears.

The singularity in the solution (A3) tends to the ordinary fluid dynamics singularity ($m = \frac{1}{2}$) as the magnetic field tends to zero.

As an example, it is instructive to look at the solution (A3) for the flow past a flat plate at the incidence α, applying the uniqueness condition at the trailing edge. The solution gives

$$(p_t - p_b) = 2\rho_0 u_0^2\alpha(-\nu)(\mu^2+\nu^2)^{-1}(\sin\pi m_2)^{-1}[(1-x)/(1+x)]^{1-m_2} \tag{A7}$$

The pressure singularity near the leading edge is reduced by the magnetic field since $m_2 > \frac{1}{2}$.

For the symmetric body, the solution for boundary values of the fluid component w of velocity is given by

$$(w)_t = -(w)_b = -\frac{1}{\nu_1^2+\mu_1^2}\left\{\mu_1 K(x) + \frac{\nu_1}{\pi}(1+x)^{m-1}(1+x)^{-m}\times \int_{-1}^{1}(1+s)^{1-m}(1-s)^m(s-x)^{-1}K(s)ds\right\} + c_1(1+x)^{m-1}(1-x)^m \tag{A8}$$

where

$$\mu_1 = \lambda_1 M_0^{-1}b^{-1} + b(M_0^2+t^2)(1+\lambda_1^2)(t^2+\lambda_1^2)^{-1} \tag{A9a}$$

$$\nu_1 = b\lambda_1 t^{-1}(\lambda_1^2 - M_0^2)(1-t^2)(t^2+\lambda_1^2)^{-1} \tag{A9b}$$

$$m = m_1 = (1/\pi)\tan^{-1}(\nu_1/\mu_1) \qquad 0 < m_1 < \tfrac{1}{2} \tag{A9c}$$

$$K(x) = \lambda_1 b^{-1}M_0^{-2}(1+b^2+b^2M_0^2)\zeta_0 + \{(M_0^2+t^2)(1+\lambda_1^2-M_0^2)(t^2+\lambda_1^2)^{-1} - \lambda_1 M_0^{-1}\}k(x) + \frac{\lambda_1}{\pi t}(\lambda_1^2 - M_0^2)(1-M_0^2-t^2)(t^2+\lambda_1^2)^{-1}\times \int_{-1}^{1}k(\xi)(\xi-x)^{-1}d\xi \tag{A9d}$$

and ζ_0 is the constant value of ζ on the body. Here the Kutta condition is applied at the leading edge.

Appendix B

The equations leading to the derivation of the integral equation in the hyperliptic restricted problem are set out. The real Riemann invariant is given by (16), which, with $b = 0$, may be written as $\mathbf{r}\cdot\mathbf{P}$, where

$$\mathbf{P} = (\sigma/m_0^2, v, \xi, \eta) \tag{B1}$$

$$\mathbf{r}(\lambda) = \{(1-m_0^2)\cos\theta + \lambda\sin\theta, \lambda\cos\theta - \sin\theta, 1 - [m_0^2/(1+\lambda^2)], \lambda[m_0^2/(1+\lambda^2) - 1]\} \tag{B2}$$

λ_1 is taken to correspond to the characteristic defining the domain of dependence in the lower half-plane and λ_4 in the upper. Let $\mathbf{c}$ be $\mathbf{r}(\lambda_1)$ and $\mathbf{d}$ be $\mathbf{r}(\lambda_4)$. The complex Riemann invariant Z_2 is obtained from (B1) with $\lambda = s + it$ and may be expressed in terms of its real and imaginary parts as

$$Z_2 = W_1 + W_2 = (\mathbf{a} + i\mathbf{b})\cdot\mathbf{P} \tag{B3}$$

where

$$\mathbf{a} = \{(1 - m_0^2)\cos\theta + s\sin\theta,\quad s\cos\theta - \sin\theta,\quad 1 - m_0^2(1 + s^2 - t^2)/D,\quad s[m_0^2(1 + s^2 + t^2) - 1]/D\} \tag{B4a}$$

$$\mathbf{b} = \{t\sin\theta,\ t\cos\theta,\ 2st\,m_0^2 D,\quad t[m_0^2(1 - s^2 - t^2) - 1]/D\} \tag{B4b}$$

$$D = (1 + s^2 - t^2) + 4s^2t^2 \tag{B4c}$$

By the elimination procedures described, one integral equation for the unknown function $F(x)$ may be obtained:

$$\mu F(x) + \frac{\nu}{\pi}\int \frac{F(\rho)}{\rho - x}\,d\rho = k(x) \tag{B5}$$

where

$$\mu = (a_1b_3 - a_3b_1)(c_1d_4 + c_4d_1) + (a_4b_1 - a_1b_4)(c_1d_3 + c_3d_1) + 2c_1d_1(a_3b_4 - a_4b_3) \tag{B6a}$$

$$\nu = (c_3d_1 - c_1d_3)(a_1a_4 + b_1b_4) - (c_4d_1 - c_1d_4)(a_1a_3 + b_1b_3) - (a_1^2 + b_1^2)(c_3d_4 - c_4d_3) \tag{B6b}$$

and $k(x)$ is a known function.

Appendix C

Details of the completed integral equation in the general two-dimensional problem are given. The coefficients of the invariants associated with the quadratic factor are renamed to avoid confusion:

$$\mathbf{r}_+ = \mathbf{e} \tag{C1a}$$

$$\mathbf{r}_- = \mathbf{f} \tag{C1b}$$

The coefficients of the other two real invariants are also renamed:

$$\mathbf{r}_1 = \cos\phi_1\mathbf{c} \tag{C2a}$$

$$\mathbf{r}_4 = \cos\phi_4\mathbf{d} \tag{C2b}$$

and for the complex invariants

$$\mathbf{r}_2/\cos\phi_2 = (\mathbf{a} + i\mathbf{b}) \tag{C3}$$

where $\mathbf{a}$ and $\mathbf{b}$ are real. It is easily verified that $\mathbf{a}$ and $\mathbf{b}$ are given by

$$\mathbf{a} = \{M_0^2 s(1 + s^2 + t^2)/D - \sin\theta(\cos\theta + \sin\theta),\ 1 - M_0^2(1 + s^2 - t^2)/D,\quad [(1 + s^2 - t^2)(s\cos\theta - \sin\theta) + 2st^2\cos\theta]/D,\quad -sa_3 + tb_3,\quad bs(1 + s^2 + t^2)/D,\quad b\sin\theta\} \tag{C4a}$$

$$\mathbf{b} = \{M_0^2 t(1 - s^2 - t^2)/D - t\sin^2\theta,\quad 2st/D,\quad [t\cos\theta(1 - s^2 - t^2) + 2st\sin\theta]/D,\ -(ta_3 + sb_3),\quad bt(1 - s^2 - t^2)/D,\quad 0\} \tag{C4b}$$

The matrices A, B of (22) are given by

$$\begin{aligned}
A_{11} &= -2M_1c_6d_1 + M_2a_6b_1 - M_3a_6d_1 + 2M_4e_6f_1\\
A_{12} &= 2M_1d_1(a_1c_6 - a_6c_1)/b_1 - M_2a_1a_6 - 2M_4f_1(a_1e_6 - a_6e_1)/b_1\\
A_{21} &= -2N_1c_6d_1 + M_2a_6f_1 - N_3a_6d_1 + 2N_4e_6f_1\\
A_{22} &= 2N_1d_1(a_1c_6 - a_6c_1)/b_1 - 2N_4f_1(a_1e_6 - a_6e_1)/b_1
\end{aligned} \tag{C5}$$

$$\begin{aligned}
B_{11} &= -M_2a_1a_6\\
B_{12} &= a_6(M_3d_1 - M_2b_1)\\
B_{21} &= 0\\
B_{22} &= a_6(N_3d_1 - M_2f_1)
\end{aligned}$$

The coefficients M_i in the foregoing may be obtained from determinants of the matrix

$$M = \begin{pmatrix} c_3d_1 - c_1d_3 & c_4d_1 - c_1d_4 & a_6(d_1 - c_1)\\ a_3b_1 - a_1b_3 & a_4b_1 - a_1b_4 & a_6b_1\\ a_3d_1 - a_1d_3 & a_4d_1 - a_1d_4 & a_6(d_1 - a_1)\\ e_3f_1 - e_1f_3 & e_4f_1 - e_1f_4 & e_6f_1 - e_1f_6 \end{pmatrix} \tag{C6}$$

after the omission of the row indicated by the subscript. The matrix N is obtained from M by the replacement of the second row of M by $(a_3f_1 - a_1f_3,\ a_4f_1 - a_1f_4,\ a_6f_1 - a_1f_6)$.

Appendix D

The flows due to the point and line singularities near the leading and trailing edges are evaluated in the restricted problem. With the notation of Appendix B, the flow variables are obtained from the Riemann invariants from the equation

$$\mathbf{P} = R^{-1}\mathbf{Z} = \sum_{j=1}^{4} F_{ij}Z_j \tag{D1}$$

where

$$\mathbf{Z} = (Z_1, W_1, W_2, W_4) \tag{D2}$$

and where R is the 4×4 matrix whose rows are the vectors $\mathbf{c}, \mathbf{a}, \mathbf{b}, \mathbf{d}$.

With the homogeneous boundary conditions $v_t = v_b = 0$ and the usual conditions on the real invariants, it follows that

$$(Z_4)_t = -\{f_{22}(W_1)_t + f_{23}(W_2)_t\}/f_{24} \tag{D3a}$$

$$(Z_1)_b = -\{f_{22}(W_1)_b + f_{23}(W_2)_b\}/f_{24} \tag{D3b}$$

The real invariants in the flow are given by their value traced back along a characteristic to the body. The flows for the leading and trailing edges are calculated separately, and it is convenient to take each edge in turn as the origin of coordinates. Hence, the invariants have the associated values at any point in the flow given by the following:

In the trailing edge calculation:

$$Z_1(x,y) = H(-y)H(-x - \lambda_1 y)\{Z_1(x + \lambda_1 y)\}_b \tag{D4a}$$

$$Z_4(x,y) = H(y)H(-x - \lambda_4 y)\{Z_4(x + \lambda_4 y)\}_t \tag{D4b}$$

In the leading edge calculation:

$$Z_1(x,y) = H(-y)H(x + \lambda_4 y)\{Z_1(x + \lambda_4 y)\}_b \tag{D5a}$$

$$Z_4(x,y) = H(y)H(x + \lambda_4 y)\{Z_4(x + \lambda_4 y)\}_t \tag{D5b}$$

where the body values of the invariants on the right-hand side are obtained from (D3), and $H(x)$ denotes the Heaviside function. The point singularity in the complex Riemann invariant according to (43) is

$$W_1 = r^{-n}(\cos n\psi + \gamma\sin m\psi) \tag{D6a}$$

$$W_2 = r^{-n}(\gamma\cos n\psi - \sin n\psi) \tag{D6b}$$

where r and ψ are defined by

$$z = x + iY = x + sy + ity = re^{i\psi} \tag{D7}$$

The constant γ is determined from the discontinuities in W_1 and W_2 across the body. From the relation between $F(x)$ and $G(x)$ and the homogeneous boundary condition on v, it follows that

$$b_1\{(W_1)_t - (W_1)_b\} = a_1\{(W_2)_t - (W_2)_b\} \tag{D8}$$

Hence, from (D7), for a trailing edge calculation ($\psi_t = \pi$, $\psi_b = -\pi$)

$$\gamma = -a_1/b_1 \tag{D9}$$

and for a leading edge calculation ($\psi_t = 0$, $\psi_b = 2\pi$)

$$\gamma = \frac{-a_1 \sin 2\pi n + b_1(1 - \cos 2\pi n)}{a_1(1 - \cos 2\pi n) + b_1 \sin 2\pi n} \qquad \text{(D10)}$$

The flow variable vector **P** now may be obtained from the above equations. A point

$$x = k(\phi)\cos\phi \qquad y = k(\phi)\sin\phi$$

is chosen, and thus

$$\psi = \arctan\{t \sin\phi/(\cos\phi + s \sin\phi)\}$$

$$r = k\{(\cos\phi + s \sin\phi)^2 + t^2 \sin^2\phi\}^{1/2}$$

The real and imaginary invariants are evaluated and substituted in (D1) for **P**. The variables ζ and v are given directly, and u is obtained from the relation (3). The ratio v/u for the streamline diagrams discussed in Sec. 6 is seen to be independent of k and r and is a function of ϕ only. A similarity flow thus is obtained.

References

[1] Sears, W. R. and Resler, E. L., "Theory of thin airfoils in fluids of high electrical conductivity," J. Fluid Mech. **5**, 257 (1959); also McCune, J. E. and Resler, E. L., "Compressibility effects in magnetoaerodynamic flows past thin bodies," J. Aerospace Sci. **27**, 493 (1960).

[2] Grad, H., "Reducible problems in magneto-fluid dynamic steady flows," Revs. Mod. Phys. **32**, 830 (1960).

[3] Cumberbatch, E., Sarason, L., and Weitzner, H., "A magnetofluid-dynamic Kutta-Joukowsky condition," J. Aerospace Sci. **29**, 244 (1962).

[4] Mikhlin, S. G., *Integral Equations* (Pergamon Press, New York, 1957), p. 126.

[5] Stewartson, K., "Magneto-fluid dynamics of thin bodies in oblique fields," Z. Angew. Math. Phys. **12**, 261 (1961).

MARCH 1963 AIAA JOURNAL VOL. 1, NO. 3

Refraction Angles for Luminous Sources Within the Atmosphere

M. J. SAUNDERS[1]

Bell Telephone Laboratories, Whippany, N. J.

The preliminary tabulation of the altitude variation of atmospheric density computed by the Air Research and Development Command (1959 ARDC model atmosphere) is used to integrate numerically the equation of atmospheric refraction. The refraction angles are obtained as functions of the altitude and apparent zenith angle of a luminous source and agree, at large altitudes and at zenith angles up to 86°, with Bessel's astronomical values (maximum discrepancy being 2 out of 726 sec of arc). This study also determines the height of the atmosphere, for refraction considerations, to be 26 ± 1 miles.

ASTRONOMICAL refraction refers to the refraction of a ray of light as it passes from a celestial object to the eye of the observer. The angle of astronomical refraction is the angular difference between the true direction of the celestial object and its apparent direction (Fig. 1). The cause of this refraction is the altitude variation of the atmospheric density, for it is well known that a ray of light will be bent as it travels between media of different densities if the angle of incidence at the interface has any value other than zero. It is also well known that the angle of astronomical refraction depends upon the zenith angle of the source and the temperature and pressure at the site of the observer, and a large effort has been devoted to the determination of the relationship between these quantities.[2] It will be shown that the most important relationship needed to obtain the theoretical values of the astronomical refraction angles is that between atmospheric density and the height above the earth's surface. The tables of Bessel (3),[3] giving the values of the astronomical refraction angle as functions of the apparent zenith angle of a celestial body and the temperature and pressure at the observer's site, are among the most reliable tables known,[4] since the theoretical values were altered so as to agree with observational results.[5]

It is, of course, apparent that refraction effects will occur for luminous sources that are located within the sensible atmosphere, and, in fact, it is just this subject with which the investigations to be described are concerned. The necessity of knowing the refraction effect for a source within the atmosphere is apparent if optical methods are employed to determine the tracking accuracy of a radar unit. Fig. 2 indicates the systematic angular errors that may be present in a combined radar-optical system. This figure shows that the total radar pointing error angle θ_t is, if boresight and parallax errors are eliminated, equal to the sum of the angle of atmospheric optical refraction θ_R and the angle between the telescope optical axis and the ray entering the optical system θ_M. The angle θ_M is the angle obtained by either a boresight camera or an optical tracker. Consequently, a measurement of θ_M and a knowledge of θ_R allows the radar error angle to be obtained. This last angle is, essentially, composed of two parts: one due to the radar servo errors and the other due to radar atmospheric refraction. This implies that the value of the angle of radar atmospheric refraction is needed only if the error due to the radar servo is desired. If, however, one is interested in the value of the total radar pointing error, then the angle of atmospheric optical refraction is the only refraction angle needed, and it is obvious that an accurate determination of θ_t requires that the refraction angle be determined accurately.

Received by ARS August 28, 1962; revision received October 2, 1962.

[1] Member of Technical Staff, Engineering Mechanics Department.

[2] The names of Bessel, Ivory, and Bouger are intimately associated with this subject. Their investigations, particularly those of Bessel, are collected in Refs. 1 and 2.

[3] Numbers in parentheses indicate References at end of paper.

[4] Another well-known table is the Poulkova Table, published in 1870 by Glyden.

[5] The methods whereby the refraction angles are determined experimentally are given by Olmstead (4).